



**DESIGN AND IMPLEMENTATION OF A FATIGUE TESTING
MACHINE FOR WELDED PARTS**

GİZEM ÇELEBİ

FEBRUARY 2020

DESIGN AND IMPLEMENTATION OF A FATIGUE TESTING
MACHINE FOR WELDED PARTS

A THESIS SUBMITTED TO
THE GRADUATE SCHOOL OF NATURAL AND APPLIED SCIENCES
OF
ÇANKAYA UNIVERSITY

BY
GİZEM ÇELEBİ

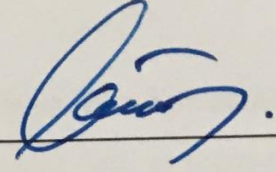
IN PARTIAL FULFILLMENT OF THE REQUIREMENTS FOR THE
DEGREE OF
MASTER OF SCIENCE
IN
MECHANICAL ENGINEERING
DEPARTMENT

FEBRUARY 2020

Title of the Thesis: **Design and Implementation of a Fatigue Testing Machine for Welded Parts**

Submitted by **Gizem ÇELEBİ**

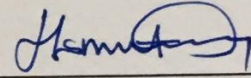
Approval of the Graduate School of Natural and Applied Sciences, Çankaya University.



Prof. Dr. Can ÇOĞUN

Director

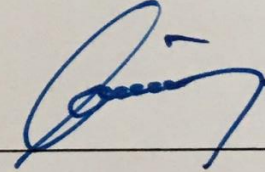
I certify that this thesis satisfies all the requirements as a thesis for the degree of Master of Science.



Prof. Dr. Haşmet TÜRKOĞLU

Head of Department

This is to certify that we have read this thesis and that in our opinion it is fully adequate, in scope and quality, as a thesis for the degree of Master of Science.



Prof. Dr. Can ÇOĞUN

Supervisor

Examination Date: 07.02.2020

Examining Committee Members

Prof. Dr. Can ÇOĞUN

(Çankaya Univ.)

Assoc. Prof. Dr. Gökhan KÜÇÜKTÜRK

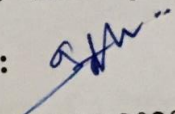
(Gazi Univ.)

Asst. Prof. Dr. O. Selim TÜRKBAS

(Gazi Univ.)

STATEMENT OF NON-PLAGIARISM PAGE

I hereby declare that all information in this document has been obtained and presented in accordance with academic rules and ethical conduct. I also declare that, as required by these rules and conduct, I have fully cited and referenced all material and results that are not original to this work.

Name, Last Name : Gizem ÇELEBİ
Signature : 
Date : 11.02.2020

ABSTRACT

DESIGN AND IMPLEMENTATION OF A FATIGUE TESTING MACHINE FOR WELDED PARTS

ÇELEBİ, Gizem

M.Sc., Department of Mechanical Engineering

Supervisor: Prof. Dr. Can ÇOĞUN

January 2020, 45 pages

In this study, the design, manufacturing and implementation steps of a fatigue test machine for the welded parts of the BOZANKAYA Inc. was given. Fatigue experiments were performed to test the designed machine by using different welded parts of BOZANKAYA Inc. busses. The S-N and log(S-N) curves were plotted by using the fatigue test results obtained. The welded parts with different geometry and size can be tested successfully by using the machine.

Keywords: Fatigue Bending Test Machine, Welded Parts.

ÖZ

**KAYNAKLI PARÇALAR İÇİN YORULMA TEST CİHAZI TASARIMI VE
UYGULAMASI**

ÇELEBİ, Gizem

Yüksek Lisans, Makine Mühendisliği Anabilim Dalı

Tez Yöneticisi: Prof. Dr. Can ÇOĞUN

Ocak 2020, 45 sayfa

Bu tez çalışmasında, BOZANKAYA A.Ş. bünyesinde bulunan kaynaklı parçalar için yorulma test cihazı tasarımı, imalatı ve uygulama aşamaları sunulmuştur. BOZANKAYA A.Ş tarafından üretilen otobüslerin kaynaklı parçalar kullanılarak, tasarlanan makinenin test edilmesi için yorulma deneyleri gerçekleştirilmiştir. Elde edilen yorulma test sonuçları kullanılarak S-N ve log(S-N) eğrileri çizilmiştir. Farklı geometri ve ebatlara sahip kaynaklı parçalar yorulma test makinesi kullanılarak başarıyla test edilebilmektedir.

Anahtar Kelimeler: Yorulma Eğme Test Makinesi, Kaynaklı Parçalar.

ACKNOWLEDGEMENT

In the realization of this study I would like to thank and express my sincere gratitude to my thesis supervisor, Prof. Dr. CAN OĐUN who shared his valuable knowledge with me and devoted valuable time whenever I consulted him.

I would like to thank the assistance of Prof. Dr. MÜFİT GÜLGEÇ who offered me valuable suggestions for this study.

I extend my sincere thanks to the BOZANKAYA Inc. authorities who supported me in doing this work. Also, I would like to thank Okan ASLAN, the foreman of the profile processing department in Bozankaya Inc, for his support throughout the study.

TABLE OF CONTENTS

STATEMENT OF NON-PLAGIARISM PAGE	i
ABSTRACT	iv
ÖZ	iv
ACKNOWLEDGEMENT	vi
TABLE OF CONTENTS	vii
LIST OF FIGURES	ix
LIST OF TABLES	xi
CHAPTERS:	
1.INTRODUCTION	1
1.1 Bending Fatigue	1
1.2 Welding Life Tests	4
1.2.1 Destructive Weld Testing	4
1.2.2 Non-Destructive Weld Testing	6
2.PURPOSE	7
3. THEORY	8
3.1 Basic Concepts of Metal Fatigue.....	9
3.2 Types of Fatigue	11
3.2.1 High Cycle (Low Strain) Fatigue	12
3.2.2 Low Cycle (High Strain) Fatigue	12
3.3 Fatigue Damage.....	13

3.3.1 Crack Formation	14
3.3.2 Crack Propagation.....	15
3.3.3 Fatigue Fracture	15
3.4 Fatigue Life Calculation Methods	16
3.4.1 S-N (Stress Life)	17
4.EXPERIMENTAL STUDIES.....	21
4.1 Test Equipment Design	21
4.2 Test Equipment Characteristics	21
4.2.1 Hydraulic Power Unit	25
4.2.2 Electric Control Panel.....	26
4.2.3 Inductive Sensor	28
4.2.4 Adjustable Hydraulic Piston Mounting Plate	28
4.2.5 Vise	30
5. TESTING OF THE MACHINE	31
5.1 Description of the Part and the Used Welding Parameters	31
5.2 Testing Procedure	33
5.3 Stress Calculations For The Tested Sample	34
5.4 Test Results	37
6. CONCLUSION	42
7. REFERENCES.....	43

LIST OF FIGURES

Figure 1: Rotating Bending Fatigue Test Machine	2
Figure 2: Four Point Bending Fatigue Test Machine	3
Figure 3: Resonant Bending Fatigue Test Machine	3
Figure 4: Axial Fatigue Test Machine	4
Figure 5: Fatigue Damage Due to Torsional Loading	9
Figure 6: S-N Diagram (Wöhler)	9
Figure 7: Basic Concepts of Metal Fatigue (a) A typical stress-time curve and (b)Tension/Compression Loading, Tension Loading.....	11
Figure 8: High Cycle (low strain) Fatigue (HCF)	12
Figure 9: Low Cycle (high strain) Fatigue (LCF)	13
Figure 10: Typical Fatigue Fracture Surface	14
Figure 11: Fatigue Crack Initiation	14
Figure 12: Fracture Progress in the Perpendicular Direction	15
Figure 13: Fatigue Fracture (a) Surface of a Fatigue Fracture (b) SEM Images of Fatigue Fracture	16
Figure 14: S-N Curve-Linear Scale	17
Figure 15: S-N Curve-Logarithmic Scale	18
Figure 16: Tensile Stress, Yield Stress and Endurance Limit on SN Curve	18
Figure 17: S-N Curve-Infinite Life Zone	19
Figure 18: Elastic Region	20
Figure 19: Plastic Region	20
Figure 20: Fatigue Testing Machine Schematic Drawing.....	23
Figure 21: The Fatigue Testing Machine	24
Figure 22: The Hydraulic Power Unit.....	25
Figure 23: Electrical Wiring Diagram of the System.....	27
Figure 24: Electric Control Panel.....	27
Figure 25: Inductive Sensor Image	28

Figure 26: Adjustable Hydraulic Piston Mounting Plate (a) 3D Design (b, c) The Manufactured System (Side and Front Views)	29
Figure 27: The Vise (a) Top View (b) The Vise with a Fixed Sample	30
Figure 28: The Sample Part Used in the Tests	31
Figure 29: Welded Samples for Fatigue Testing.....	32
Figure 30: The MIG Welding Machine	33
Figure 31: Fillet Welds under Primary Shear and Bending Load (t = weld width, mm, b = weld length, mm, l = lever arm length, mm, d =plate thickness, mm, V = applied force, N, τ = shear stress, MPa)	35
Figure 32: Test Results (a) A Fractured Sample (104 MPa) (b) Optical Image of Failed Weld Region (“x10” Magnification).....	37
Figure 33: Stress-Strain Diagram Obtained from Fatigue Test.....	39
Figure 34: Endurance Limit in log (S-N) Diagram	40
Figure 35: Plastic, Elastic and Infinite Life Regions	41

LIST OF TABLES

Table 1: Electric Motor Characteristics of Fatigue Machine	26
Table 2: Material Specification of the Sample and Welding Wire	32
Table 3: Fatigue Test Results of the Specimens.....	38



CHAPTER 1

1. INTRODUCTION

1.1 Bending Fatigue

Fatigue is called a crack or tear that occurs on the surface of a part as a result of repeated different loads and vibrations. Fatigue tests are performed by axial loading or bending and as a result, tensile and compressive stresses occur. The bending process continues until the material is fatigued. The number of cycles (N) before the material breaks are recorded and plotted against the bending stress (S). The nominal S-N curves are obtained from the fatigue test data, mainly from axial and bending tests [1, 2].

Fatigue test machines are used to test the durability and life of the material to be tested. A wide variety of machines are used for the fatigue test process. Although the machines used in the fatigue experiment are very diverse, these machines can be mainly categorized in four groups based on the type of stresses they apply to the sample:

Machines applying;

- 1) Axial pull-push stress,
- 2) Bending stress,
- 3) Torsion stretching,
- 4) Compound stresses.

The most commonly used machines in these groups are the ones that apply bending stress whose operating principle is simple. The ones that apply planar bending stress are often used for flat products. The type and size of the sample to be used usually depends on the type, capacity and size of the machine [3]. The fatigue testing machines are classified according to the purpose of the test, load-forming mechanism, material characteristics, type of stress created in the cross-section and loading mode.

Common types of fatigue testing are as follows [4];

- 1) Rotating Bending Fatigue Test (Figure 1),
- 2) Four Point Bending Fatigue Test (Figure 2),
- 3) Resonant Bending Fatigue Test (Figure 3),
- 4) Axial Fatigue Test (Figure 4),
- 5) Repeated Bending Fatigue Test.

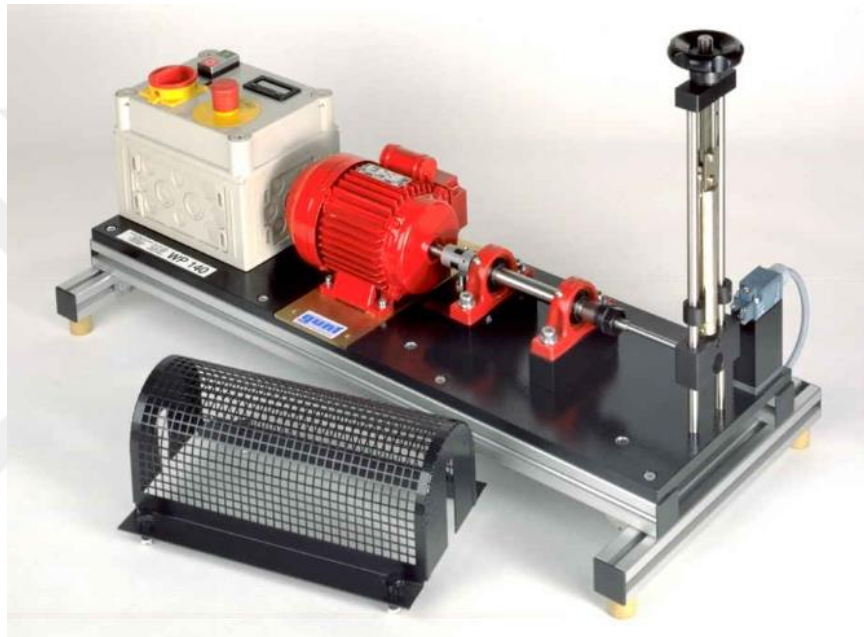


Figure 1: Rotating Bending Fatigue Test Machine [5]



Figure 2: Four Point Bending Fatigue Test Machine [6]



Figure 3: Resonant Bending Fatigue Test Machine [7]



Figure 4: Axial Fatigue Test Machine [8]

1.2 Welding Life Tests

In order to increase the quality level in welded manufacturing and to keep this level constant, it is necessary to apply testing methods. The welded parts must be subjected to non-destructive and destructive tests requested by the end user [9].

1.2.1 Destructive Weld Testing

Destructive tests are examination methods to determine the resistance and endurance against permanent shape changes [10].

Types of destructive weld testing [12];

- 1) Tensile Test
- 2) Bend Test
- 3) Hardness Test
- 4) Notch Impact Test
- 5) Macro Etch Testing

Tensile test is the most commonly used destructive material inspection method. Tensile tests are indispensable in the standards and it is quite inexpensive compared to other tests. Tensile test is used to determine the mechanical properties of materials. The tensile test is applied to identify the relationship between the strength of the welded joint and the strength of the base material used. With the tensile test, the maximum load, yield strength, tensile strength and percentage elongation characteristics of the sample can be determined [14].

Bend testing is used to measure the behavior of materials against bending forces. The bending test is used to determine ductility in butt welding and discontinuities at the weld main material interface. The purpose of the bending experiment is to determine whether the regions exposed to the bending moment of the welded region are suitable for the projected static dynamic calculations and the main material [9].

Hardness test is used to observe the change of hardness of the material after welding. Resistance of a material against a deformation is called hardness. Hardness is a test based on experience and it is not a material property [11]. According to EN 1043-1, samples taken from the main material, heat-affected region and the welding metal are tested for hardness with HV10 load [9].

Notch impact test is used to measure the impact strength of welded materials at a specific temperature. Alternating materials tend to show fragility at low temperatures. For this reason, the welded material is required to give a certain toughness values at the tested temperatures. There are two types of notch impact tests, namely, Charpy and Izod. TS EN ISO 15614 uses Charpy notch impact testing for evaluation. Additionally, in Charpy notch as well as the Izod impact and pull impact tests, the measured amount is usually the energy absorbed while breaking the sample with a single impact [13].

In Macro Etch testing, according to ISO 17639, the macro images of the samples which are cut out and prepared from the test piece are evaluated according to the same standard [9]. With this test method, throat height in corner welds, effective throat height, penetration in forehead and corner welds, and discontinuities (cracks, pores, melting deficiencies, etc.) can be determined [13].

1.2.2 Non-Destructive Weld Testing

Non-destructive material inspection is the most important part of quality control and it is the complementary part of final production. This test method provides information about dynamic and static structures. During this procedure, materials are examined without causing damage so that the test piece can be reused after inspection.

Error detection is performed with non-destructive testing method during the production of materials or after a certain period of use for reasons such as corrosion or wear cracks, internal structure of the gap, sectional reduction. In these processes, there is no need to take any samples from the materials. Tests are performed directly on the workpiece. Thus, 100% inspection of parts can be performed [14]. Non-destructive testing methods are applied in different ways, with various physical principles. The method to choose is determined by the type of material being examined and the type of error being sought.

The methods used in non-destructive testing can be listed as follows [14]:

- 1) Visual Inspection,
- 2) Liquid Penetrant Inspection,
- 3) Eddy Current Inspection,
- 4) Magnetic Particle Inspection,
- 5) Ultrasonic Inspection,
- 6) Radiographic (X-Ray) Inspection.

CHAPTER 2

2. PURPOSE

In this study,

- A bending fatigue testing machine was designed, manufactured and implemented for welded parts of Bozankaya Inc. busses,
- Some critical welded parts of the busses was selected for fatigue tests,
- Stress calculations of a tested parts were completed and a life-stress diagram (S-N) had been constructed.

By means of the constructed device, not only critical parts but also any welded parts can be tested with the fixture designed for this purpose in this study. In addition, Bozankaya Inc. owned a new fatigue tester to test its welded parts.

CHAPTER 3

3. THEORY

The simultaneous effect of cyclic stress, tensile stress and plastic stress refers to fatigue fracture. One of these three must be present for the initiation and spread of fatigue cracking [1]. ASTM standards define fatigue as “a condition caused by variable stress and shape change in a material in certain region or regions, resulting in cracks or breakages after a certain number of loads.” In the event of fatigue, cracking usually begins with a notch at the surface, a scratch, a capillary crack, or the regions where sudden cross-sectional changes occur. Figure 5 shows fatigue damage due to a torsional load. The following three main factors are usually required for crack formation [16].

- 1) A sufficiently high maximum tensile stress,
- 2) Fairly wide variation or fluctuation of applied stress,
- 3) A sufficiently large number of repetitions of applied stress.

This can be counted in a large number of side factors besides main factors. Surface quality, corrosion, temperature, overload, permanent internal stresses, compound stresses, voltage concentration, frequency, microstructure are among examples [15].

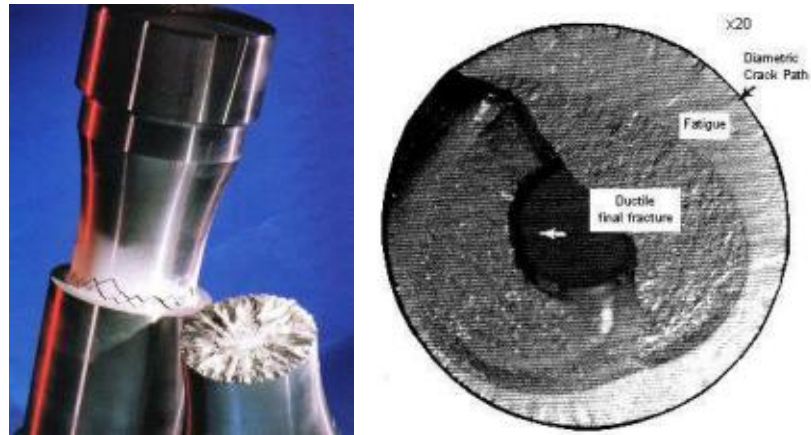


Figure 5: Fatigue Damage Due to Torsional Loading [17]

In Europe, in the beginning of the nineteenth century, fatigue damage was noticed by Wöhler. Wöhler recorded the number of cycles on which the sample was based against the constant stress value for many samples and created the S-N curve, which is still in use today (Figure 6). For each type of material and working conditions, fatigue tests are performed and a Wöhler curve is obtained. Thus, the fatigue life or the fatigue resistance of materials can be determined in advance.

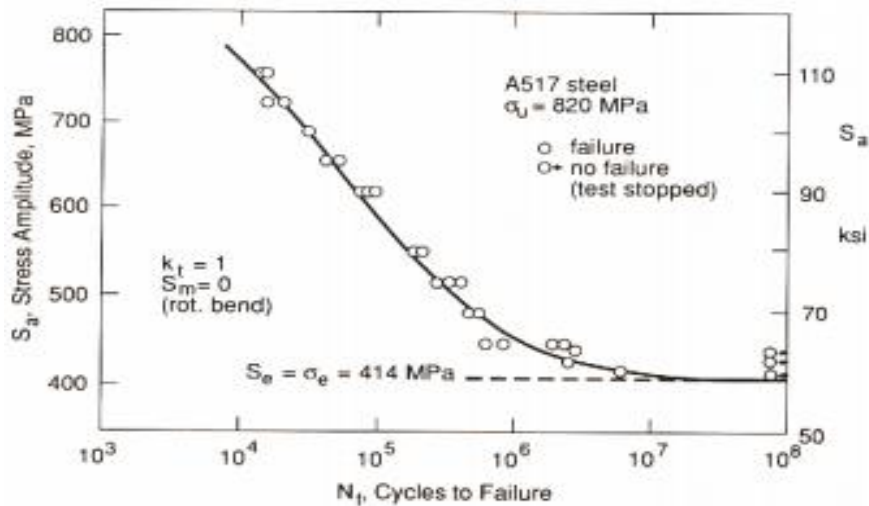


Figure 6: S-N Diagram (Wöhler) [18]

3.1 Basic Concepts of Metal Fatigue

Figure 7 shows the variation of stress causing fatigue over time and its basic parameters.

Minimum Stress (σ_{min})

The smallest stress among the applied stresses is called the minimum stress.

Maximum Stress (σ_{max})

The biggest stress among the applied stresses is called the maximum stress.

Mean Stress (σ_m)

The mean stress is equal to the half of the total of the maximum and minimum stresses.

$$\sigma_m = \frac{\sigma_{max} + \sigma_{min}}{2} \quad (1)$$

Stress Range (σ_r)

The stress range is equal to the maximum stress minus the minimum stress.

$$\sigma_r = \sigma_{max} - \sigma_{min} \quad (2)$$

Stress Amplitude (σ_a)

The stress amplitude is equal to minimum stress minus the maximum stress divided by 2.

$$\sigma_a = \frac{\sigma_{max} - \sigma_{min}}{2} \quad (3)$$

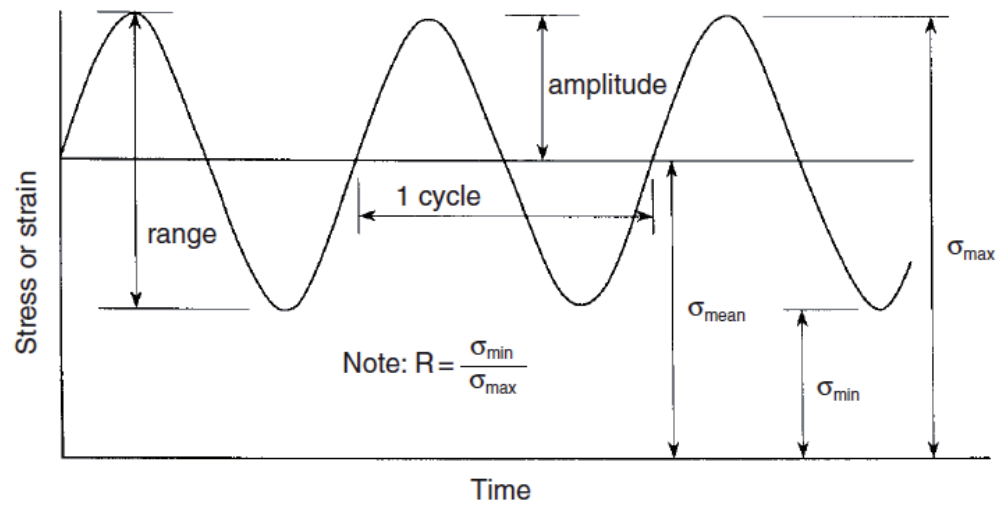
Stress Ratio

The stress ratio is the minimum stress divided by the maximum stress.

$$R = \frac{\sigma_{min}}{\sigma_{max}} \quad (4)$$

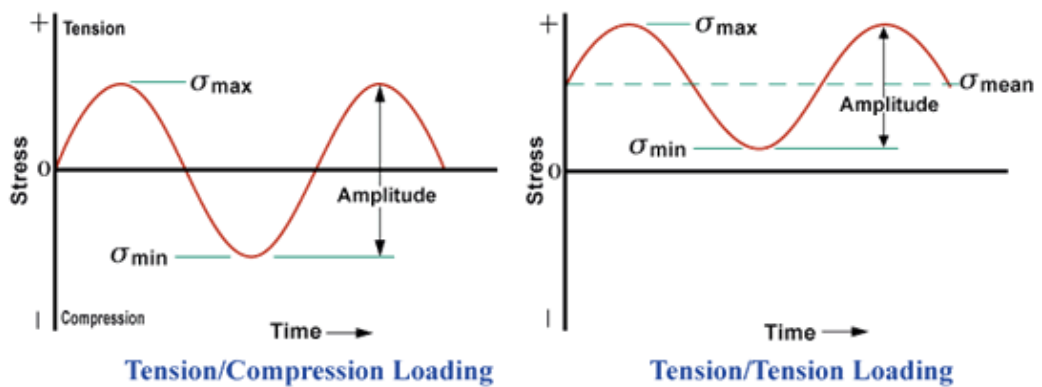
Cycle

The smallest part of the stress-time curve that is periodically repeated is called the cycle.



Time

(a)



(b)

Figure 7: Basic Concepts of Metal Fatigue (a) A typical stress-time curve
(b) Tension/Compression Loading, Tension Loading [21]

3.2 Types of Fatigue

Fatigue types under dynamic loading are divided into two parts.

- 1) High cycle (low strain) fatigue (HCF)
- 2) Low cycle (high strain) fatigue (LCF)

3.2.1 The HCF

Elastic deformation region is defined as HCF number of damage cycle (N) $> 10^5$. In case of a long-life fatigue, where the yield is out, the tension amplitude and speed are controlled. The values of σ_{min} and σ_{max} are lower than the yield strength. This type of fatigue lives are comparatively long compared to the low cycle fatigue. HCF test can be realized under load controlled waveform (Figure 8).

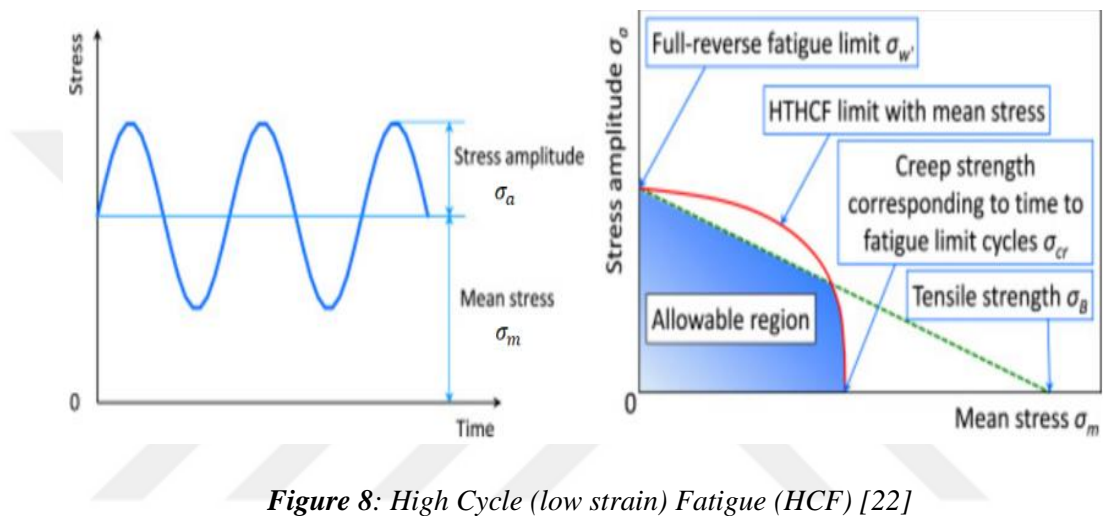


Figure 8: High Cycle (low strain) Fatigue (HCF) [22]

3.2.2 The LCF

Elastic and plastic deformation regions are defined as LCF number of damage cycle (N) $< 10^5$ (Figure 9). The σ_{min} and σ_{max} values are higher than the yield strength. Unlike the high cycle fatigue, it is controlled by unit strain amplitude, not by tensile amplitude.

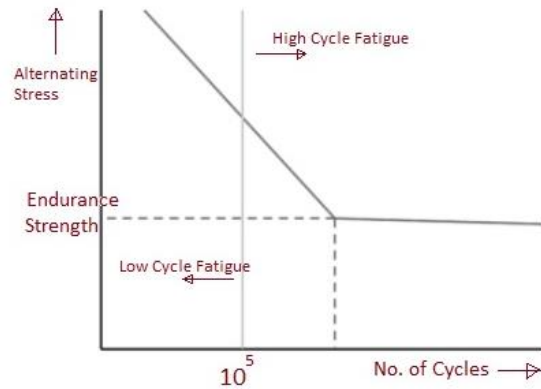


Figure 9: Low Cycle (high strain) Fatigue (LCF) [23]

3.3 Fatigue Damage

Fatigue damage occurs in the form of microcracks starting from the surface. Surface smoothness and resistance are important factors affecting the fatigue life. In addition, fatigue damage occurs as a result of a dynamic load exposure for a certain period of time. This time period varies depending on the type of the material, the quality of the surface and the size and frequency of the dynamic load. Fatigue cracks are inevitable in the process of use. Fatigue can be caused either by notches, sharp corners, indentations, protrusions and similar surface defects that disrupt surface smoothness, or residues, capillary cracks, sharp-tipped sediments and particles that disrupt uniformity within the internal structure.

Fatigue damage mechanism includes three different stages (Figure 10):

- 1) Crack Formation,
- 2) Crack Propagation,
- 3) Fatigue Fracture (Catastrophic rupture).

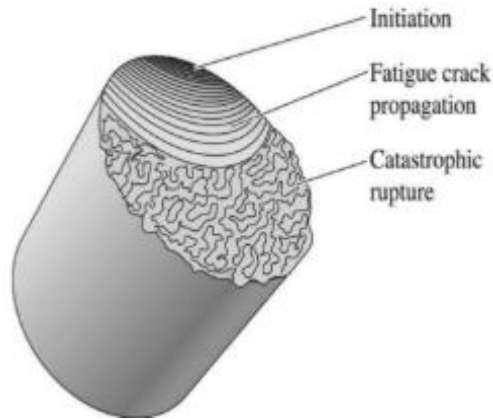


Figure 10: Typical Fatigue Fracture Surface [24]

3.3.1 Crack Formation

There are microcracks in brittle materials. If there is enough stress built up at the end of the microcrack, the microcrack advances and fracture occurs. Fatigue cracking is most likely to occur on the surface of the part since the stress reaches the maximum value on the surface. The roughness on the surface of materials acts as a notch, forming stress conglomeration (Figure 11a). Even if there is not a geometric shape to make a notch effect in ductile metals and the surface is bright enough to have no roughness, the material gets tired again. With the applied stress, dislocation movements occur on the surface grains of the metal. Due to this slippage, roughness occurs in the material, and this roughness has a notch effect again (Figure 11b) [24].

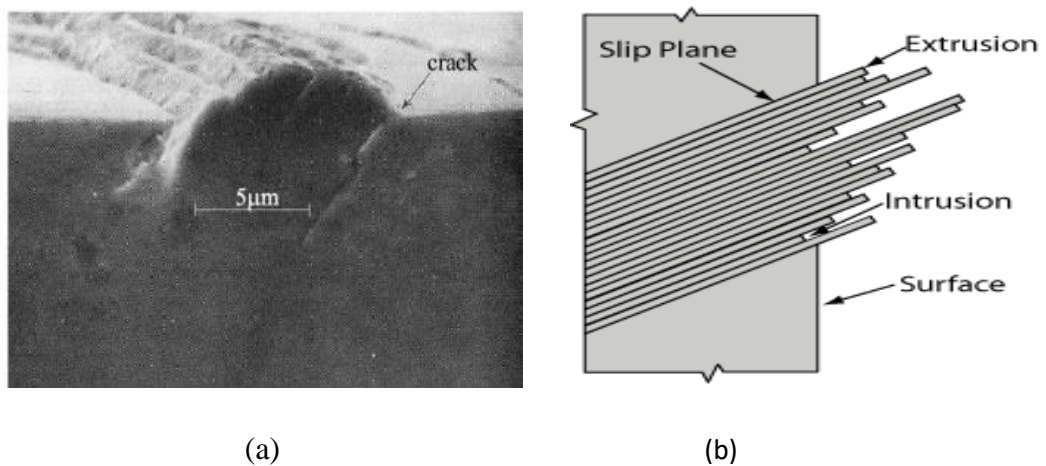


Figure 11: Fatigue Crack Initiation [21]

3.3.2 Crack Propagation

Stress must be sufficient for the progression of the crack. Otherwise the material is not fatigued. If the stress is large enough to allow the crack to move forward, the crack advances and reduces the load-bearing section of the part. This progress often continues to develop in grains by making an angle of 45° to the axis of the stress acting on the part. The crack formed as a result of the stress begins to move perpendicular to the direction of the stress and stable crack progression happens (Figure 12). Stress agglomeration in the material is effective in the process of starting the crack. The fracture toughness properties of the material gain importance during the fracture growth and fracture process [24].

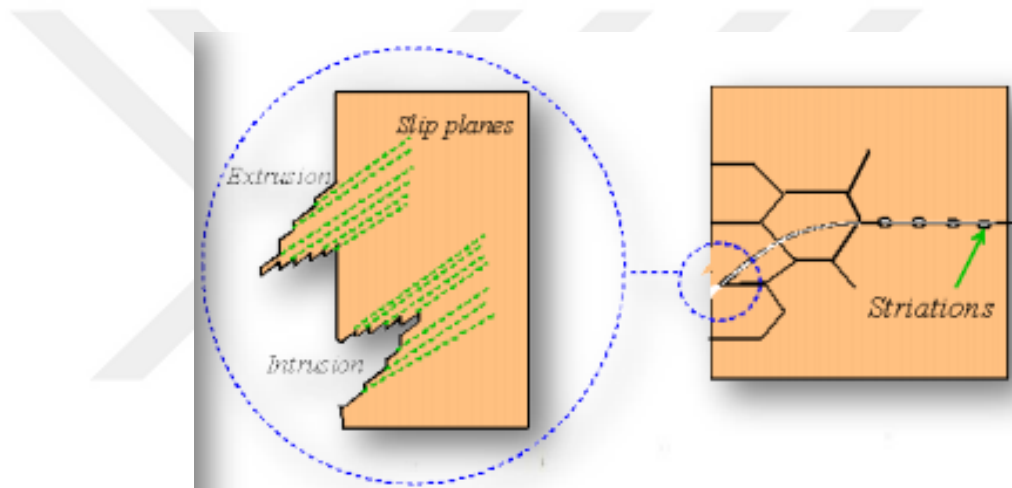
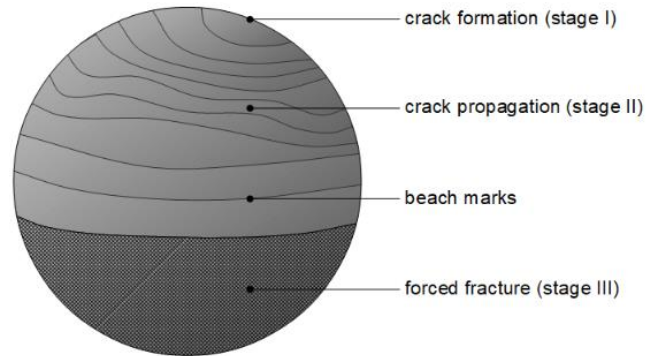


Figure 12: Fracture Progress in the Perpendicular Direction [25]

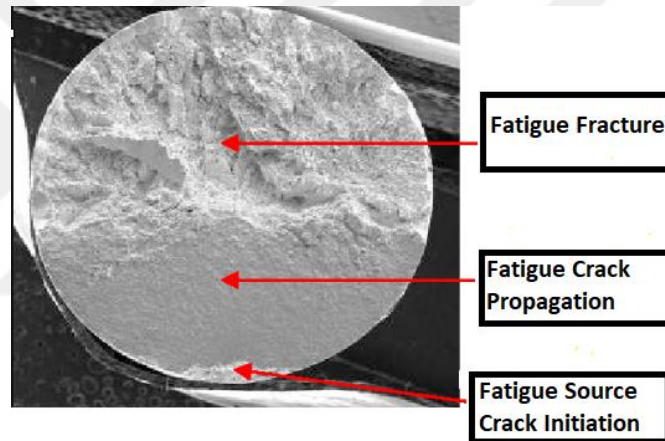
3.3.3 Fatigue Fracture

When the section shrinking with the fracture progression becomes unable to carry the applied stress, the material is broken suddenly. The surface passes through certain stages before breaking of material. Figure 13a shows the stages of a fatigue fracture. In Figure 13b, the image of this fracture is shown under Scanning Electron Microscopy (SEM). Fatigue fracture can cause a major damage, as no change in the material can be observed and the presence of the crack cannot be understood before fatigue fracture occurs. 80% of the fatigue damage is caused by mechanical damage. The fracture

surface consists of two fatigue regions. The crack propagation zone is bright while the suddenly breaking surface is rough [24].



(a)



(b)

Figure 13: Fatigue Fracture (a) Surface of a Fatigue Fracture [30] (b) SEM Images of Fatigue Fracture [26]

3.4 Fatigue Life Calculation Methods

The three most commonly used methods are as follows.

- S-N (Stress-Life)
- ϵ -N (Strain-Life)
- Linear Elastic Fracture Mechanic (Crack Propagation)

3.4.1 S-N (Stress-Life)

German scientist August Wöhler developed the S-N curve. The S-N (Wöhler) Curve shows the plot of a stress (S) against the number of cycles to failure (N) (Figure 6 and 14). This diagram gives the relationship showing how many cycles the material will crack or break under different constant stresses. The loading continues until the parts break. The S-N curve is generally accurate for lifetimes longer than 1000 cycles. The factor affecting the results in the S-N curve is not the application speed, but the number of cycles. In Figure 15, both stress and the number of cycles are shown in logarithmic or linear scales. The ordinate, which is the stress axis, is generally linear, and in some cases the logarithmic scale is used [27].

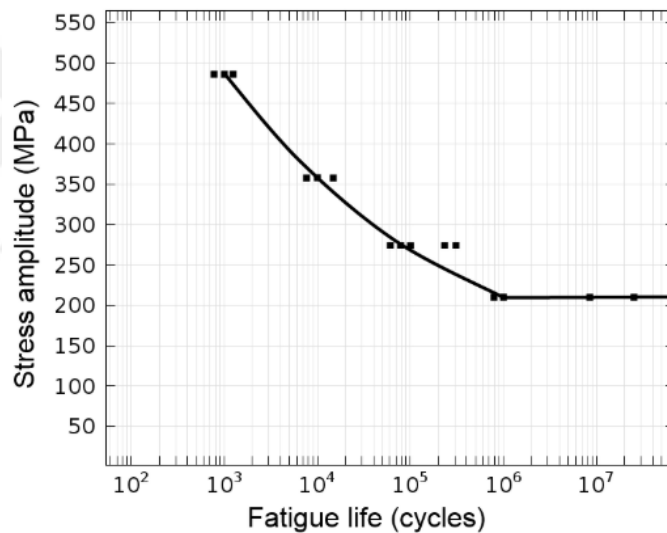


Figure 14: S-N Curve-Linear Scale [28]

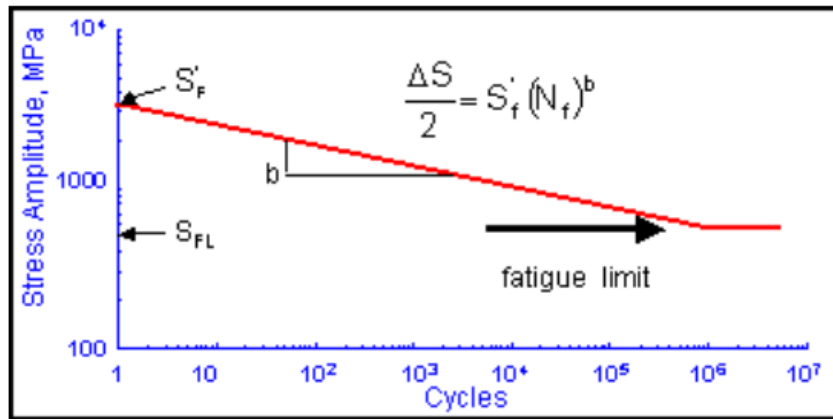


Figure 15: S-N Curve-Logarithmic Scale [27]

Plastic, Elastic and Infinite Life Zones

The plastic region, the elastic region and the infinite life regions are located in the S-N curve (Figure 16).

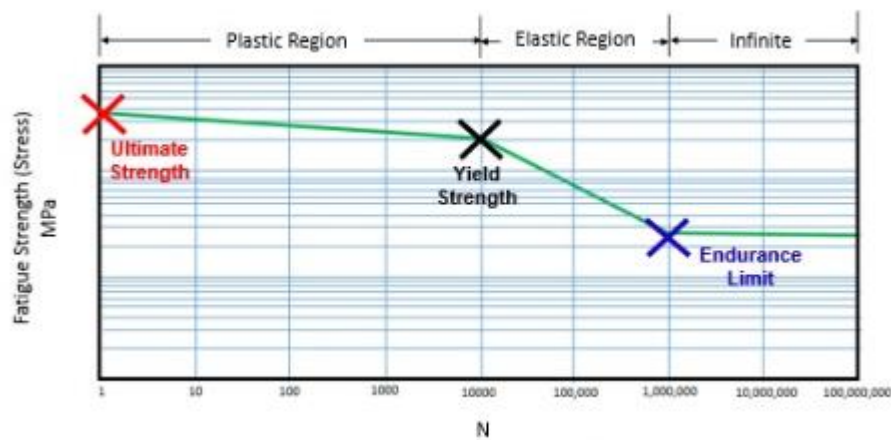


Figure 16: Tensile Stress, Yield Stress and Endurance Limit on S-N Curve [29]

Ultimate Strength: As can be seen in Figure 16, 10^0 is the maximum stress point that the materials can withstand.

Yield Strength: The yield strength refers to the separation point of the elastic and plastic regions.

Endurance Limit: The endurance limit refers to the cycle of 10^6 [29].

Infinite Life

The infinite life region is suitable for the design of critical parts such as engine crankshaft and arms (Figure 17). Cyclic stress levels that a part is subject to should be below the fatigue limit to obtain an infinite life. The infinite life ($N > 10^{6-7}$) is dependent only on the number of stress cycles. In this case, the assumption is that corrosion and other factors do not exist [29].

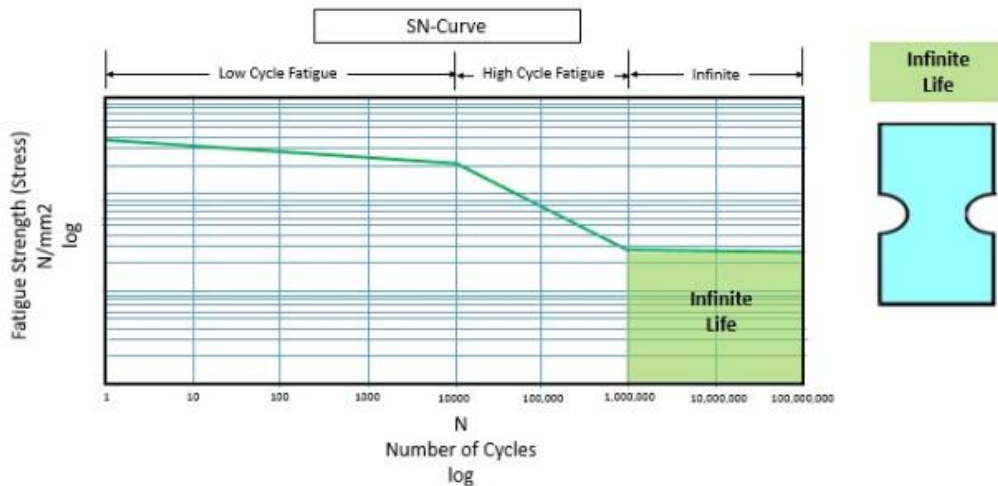


Figure 17: S-N Curve-Infinite Life Zone [29]

Elastic Region

Elastic deformation is defined as the change in shape that varies in proportion to stress. This region called the “High Cycle Fatigue” region is shown in Figure 18. The slope of this part is linear in the stress-strain curve and corresponds to the modulus of elasticity E . In the case of an application and removal of a load, the material takes its original shape or length back. Residual stress and geometric factors are among typical factors affecting the performance of a material.

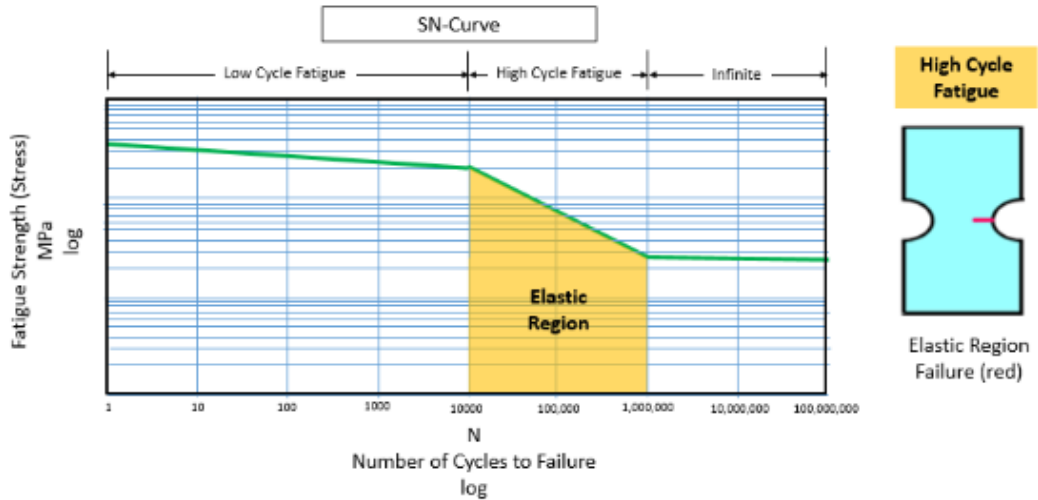


Figure 18: Elastic Region [29]

Plastic Region

Plastic deformation is a permanent one and the material in the plastic region is subjected to high stress which causes change of shape in the material. This region called the “Low Cycle Fatigue” region (Figure 19) as low numbers of stress cycle can cause a failure of the part at high amplitude. This zone is also called the high stress and low number of cycle.

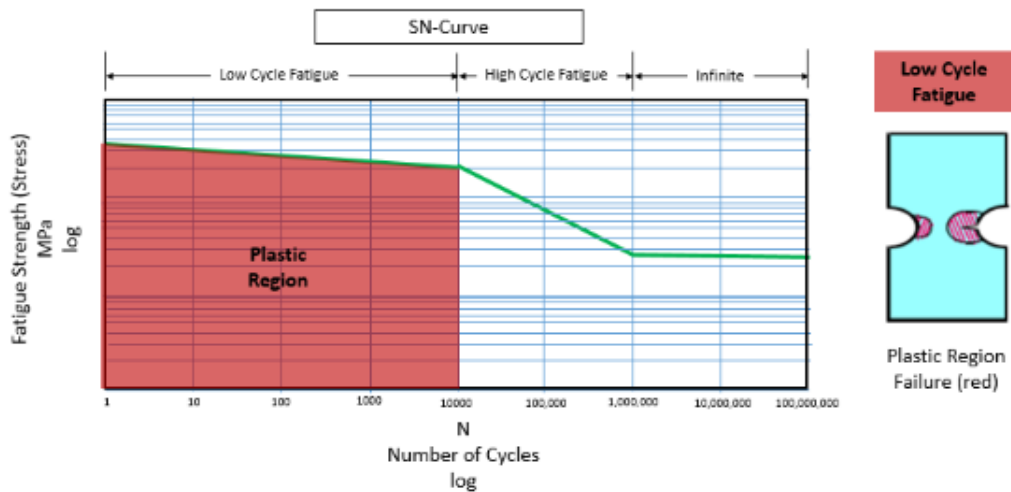


Figure 19: Plastic Region [29]

CHAPTER 4

4. EXPERIMENTAL STUDIES

4.1 Test Machine Design

In this study, a fatigue test machine for welded parts is designed and manufactured. The purpose of this thesis was to test the fatigue life of materials with this test machine. Prior to designing the machine, other fatigue test machines available in the market were examined. During the design stages of the machine, working parameters were determined as an input of the design. Firstly, the working principles of the system, hydraulic power unit capacity, hydraulic cylinder diameter, electric motor power and electric motor operating speed were determined. Another criterion of the study was the space that the test machine occupies in addition to all the other parameters mentioned. Prior to designing the fatigue test machine, it was predicted that it would be exposed to high levels of vibration during the study. In order to prevent this vibration during the tests, the body was constructed from the profiles and mounted on a thick steel plate base.

4.2 Test Equipment Characteristics

The fatigue test machine is shown schematically in Figure 20. The machine consists of a hydraulic power unit, a hydraulic piston, an adjustable hydraulic piston mounting plate, an inductive sensor, a vise and an electrical control panel. The manufactured test machine is shown in Figure 21.

The working principle of the test machine is as follows:

A hydraulic piston is used to apply the force to samples. A 380 V electric motor (1,5 kW) drives the pump of the hydraulic system. The force can be applied in a range of

3000N-12000 N. 3 strokes/s can be accomplished by the hydraulic piston and servo valves. The system is controlled by PLC control unit and inductive sensors are located at the back of the sample. These sensors generate a magnetic field in the detection range. Any metal that approaches that field, affects the field. The sensor sends a signal to the PLC control unit when the sample is broken or cracked (i.e. excessively deformed), which shuts down the power of the system. Number of cycles (N) is found by counting the signals sent to the PLC control unit from sensors. After the sample is broken, the counting stops. The control panel monitor shows the N. The touch pad on the electrical control panel is used to set the force transferred to the hydraulic cylinder.

The following precautions were taken to overcome the vibration during the operation of the machine;

- The table (1600x700 dimension) made of 15 mm sheet metal was supported with a 120x80x4 steel profile legs (Figure 20 and 21).
- An adjustable hydraulic piston mounting plate (Figure 20 and 21) was designed to apply the load to the desired position of the sample part to be tested.

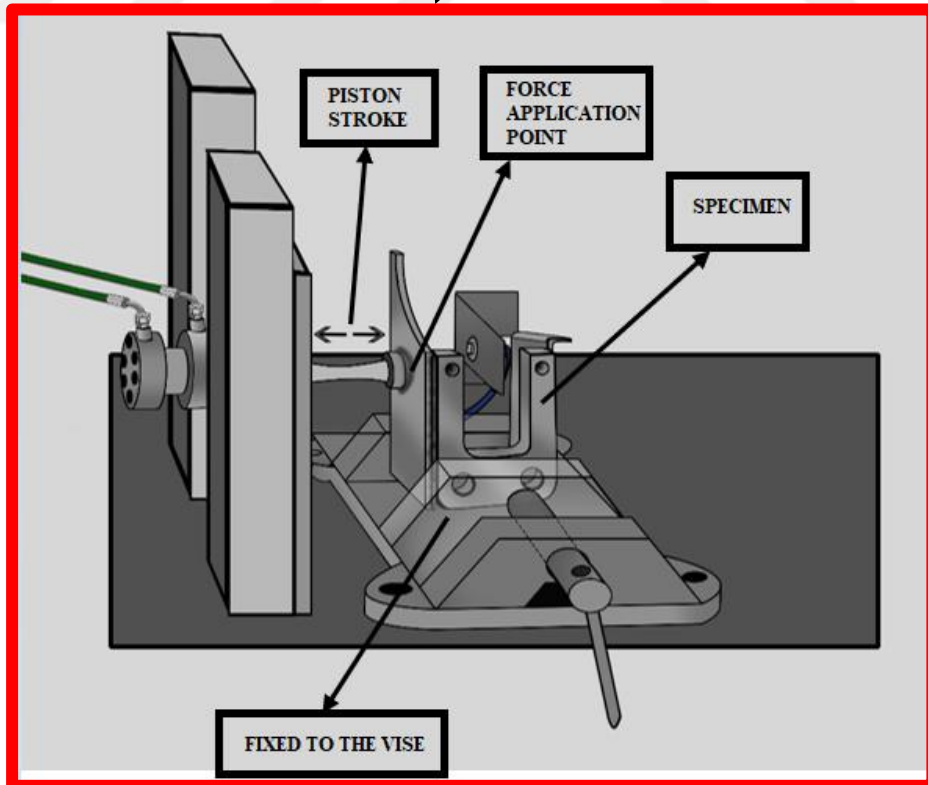
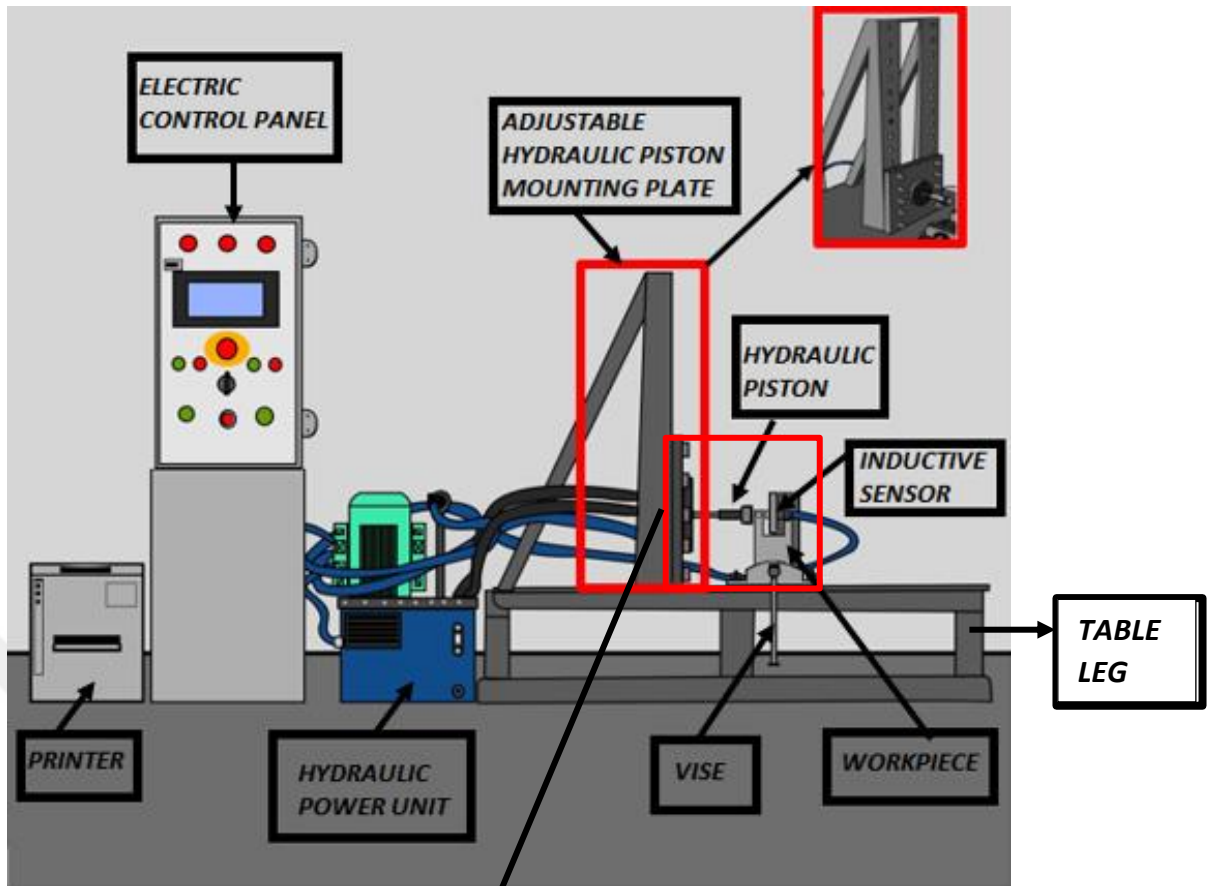


Figure 20: Fatigue Testing Machine Schematic Drawing



Figure 21: The Fatigue Testing Machine

4.2.1 Hydraulic Power Unit

The force is applied to the welded area by means of hydraulic power unit. High operating pressures are easily achieved due to the non-compressibility of liquids in a hydraulic system. Moreover, hydraulic systems are easily controlled during the operation. Hydraulic power unit consists of a tank, a pump, a motor, a filter, the safety valves, heaters and coolers, indicators and valve blocks (Figure 22). An electric motor (IE2 type) was used in the hydraulic power unit. IE2 type motor provides high efficiency operation as well as energy saving because of its high efficiency. The technical specifications of the electric motor are shown in Table 1. The hydraulic piston performs 3 strokes/s motion. The maximum applied force is 12000 N.



Figure 22: The Hydraulic Power Unit

Table 1: Electric Motor Characteristics of the Fatigue Machine

Electric Motor Technical Specifications	
Voltage (V)	380
Frequency (Hz)	50
Power (kW/HP)	1,50/ 2,00
Rotational Speed (rpm)	1430
Efficiency Class	IE2

4.2.2 Electric Control Panel

The PLC control circuit was used to record the voltage cycles during the test. It also controls the load to be applied by the user. The selected controller is compatible with the proximity sensor. The electrical wiring diagram and the Electric Control Panel are shown in Figure 23 and Figure 24, respectively.

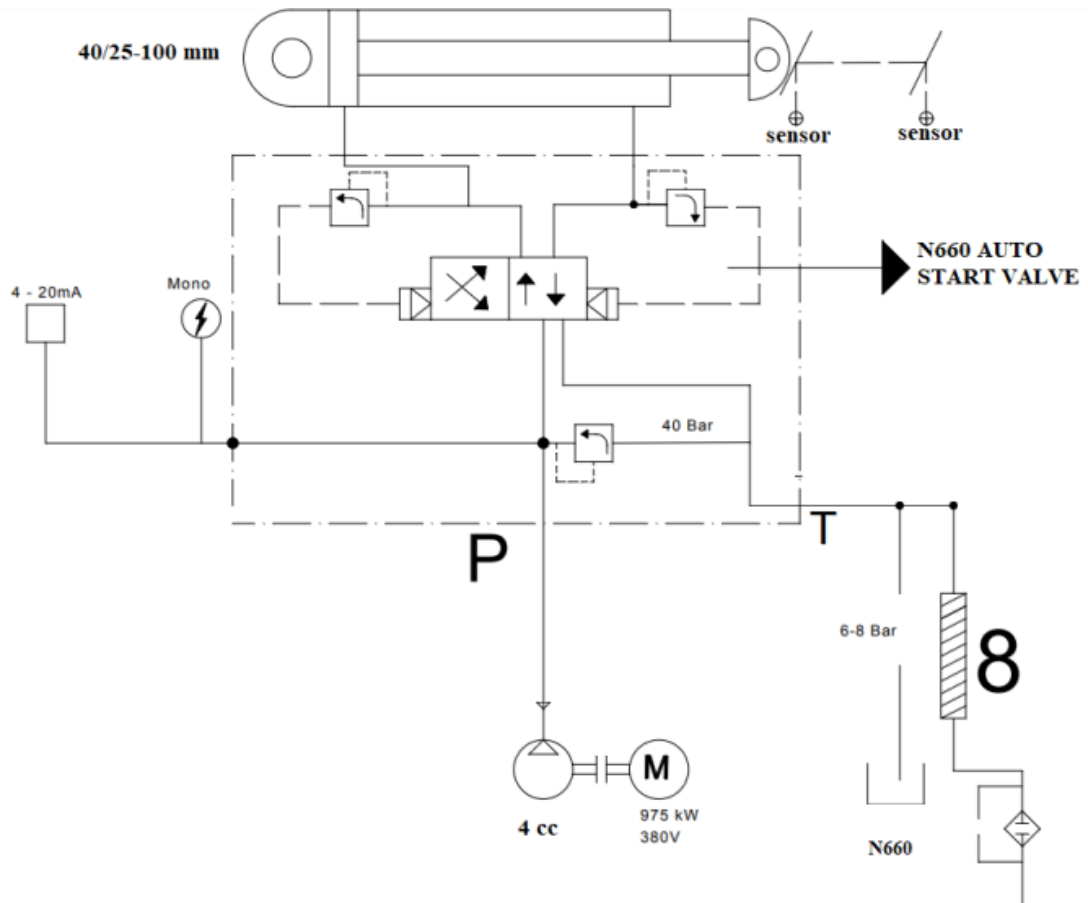


Figure 23: Electrical Wiring Diagram of the System



Figure 24: Electric Control Panel

4.2.3 Inductive Sensor

The inductive sensor (Figure 25) detects the presence of near objects without any physical contact. This situation makes it resistant to abrasion or contamination. The sensor is located just behind the welded seam of the part to be tested. The sensor is fixed to the device by means of a metal stabilizer. The sensor creates a magnetic field at detection distances when the system breaks or deforms the part.



Figure 25: Inductive Sensor

4.2.4 Adjustable Hydraulic Piston Mounting Plate

The fixing of the hydraulic cylinder is an important issue in the design phase of the fatigue test machine. The force transferred from the hydraulic cylinder must be directed correctly to the sample to be tested. The system was subjected to high vibration during operation. So, a special design was made and implemented for the hydraulic cylinder (Figure 26). The body of the hydraulic cylinder is fixed to the mounting plate with bolts. The height of the hydraulic cylinder can be adjusted by relocating the bolt positions of the mounting plate (Figure 26b) according to the size and geometry of the part. The design is fixed to the table with two supports which also minimizes the vibration of the mounting plate (Figure 26c).



(a)

**MOUNTING
PLATE**



(b)



SUPPORTS

(c)

Figure 26: Adjustable Hydraulic Piston Mounting Plate (a) 3D Design (b, c) The Manufactured System (Side and Front Views)

4.2.5 Vise

In the fatigue testing machine, a mechanical fixing device (vise) was used for clamping the samples (Figure 27). The vise was mounted to the table so that the specimen would be fixed tightly to the testing machine. The material of the vise was 1040 steel and the vise was capable of fixing different size and geometry of sample parts.

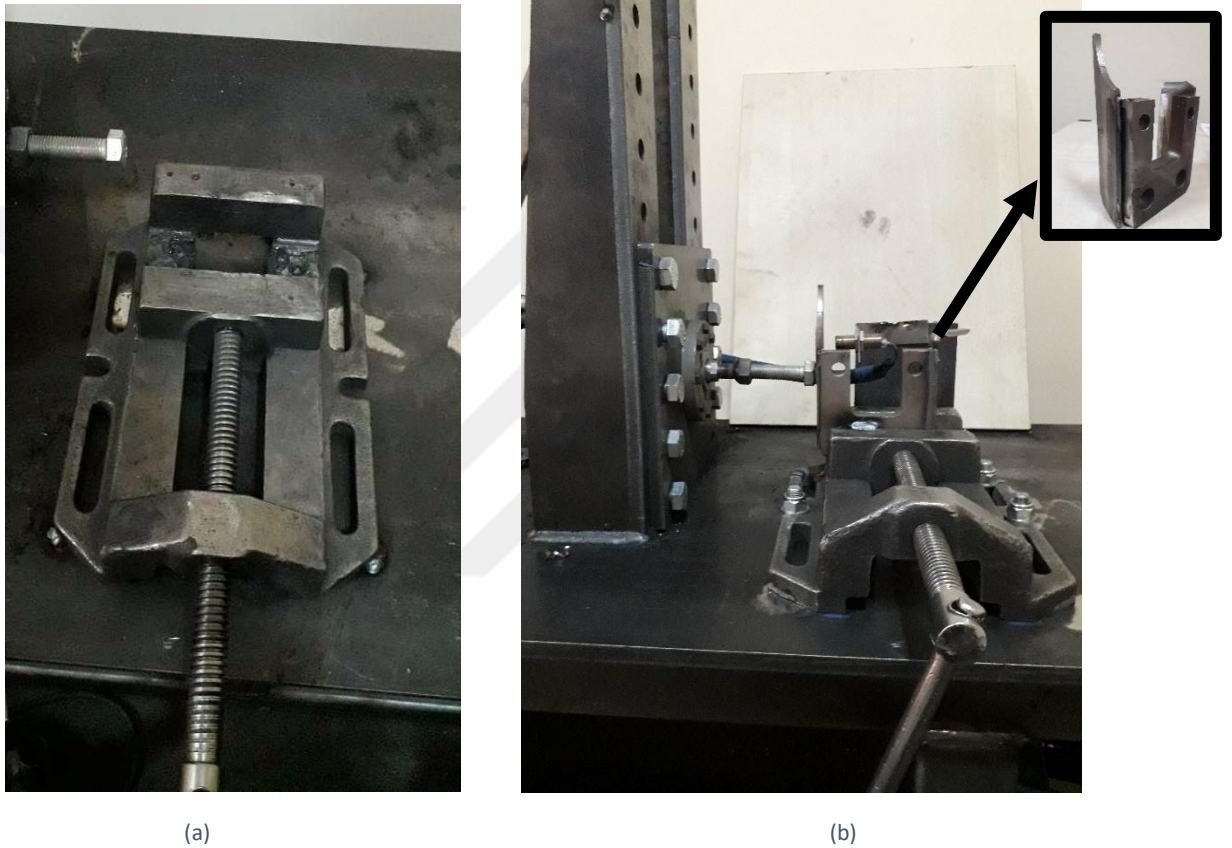


Figure 27: The Vise (a) Top View (b) The Vise with a Fixed Sample

CHAPTER 5

5. TESTING OF THE MACHINE

5.1 Description of the Part and the Used Welding Parameters

In this study, some welded test pieces produced by BOZANKAYA Inc. were used in testing of the machine.

The steel sample to be tested consisted of three pieces that were welded to each other (Figure 28). The material specifications and mechanical properties of these pieces and welding wire are presented in Table 2.

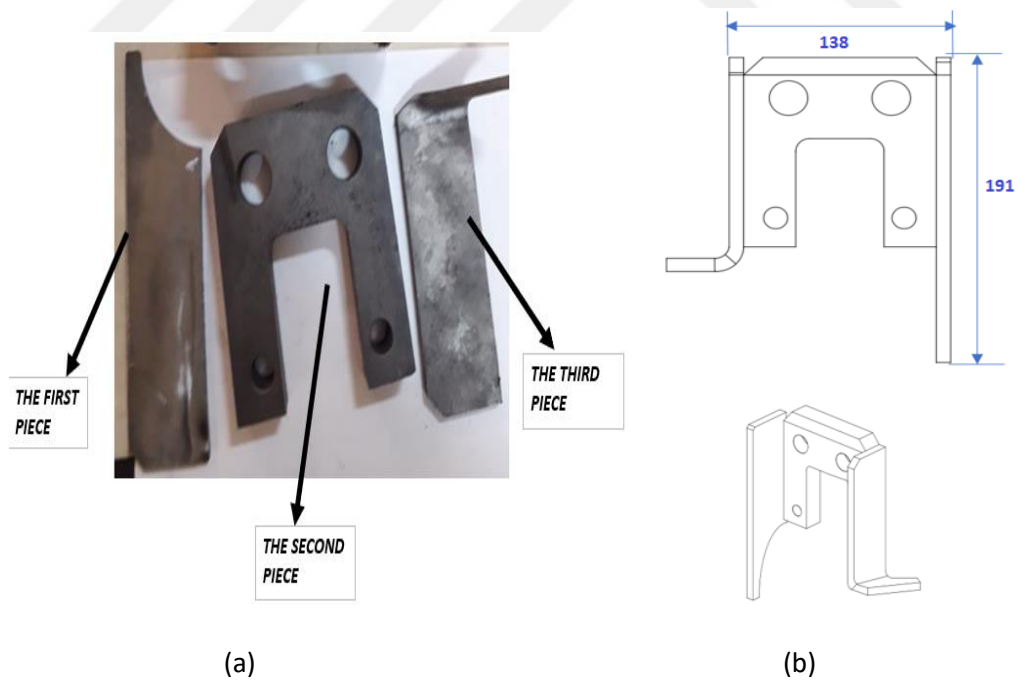


Figure 28: The Sample Part Used in the Tests

Table 2: Material Specification of the Sample and Welding Wire

USED MATERIALS	MATERIAL SPECIFICATION	TENSILE STRENGTH (MPa)	YIELD STRENGTH (MPa)
THE FIRST PIECE	Plate S355MC-ENTZ 8X1500X3000	430	355
THE SECOND PIECE	Plate St52-3N 20X1500X6000	490	335
THE THIRD PIECE	Plate S355MC-ENTZ 8X1500X3000	430	355
WELDING WIRE	St37	360	235

A total of 10 samples were used in the tests to realize the performance of the testing machine (Figure 29). These samples were welded by using the same welding machine, the welding wire, the operator and the welding parameters.

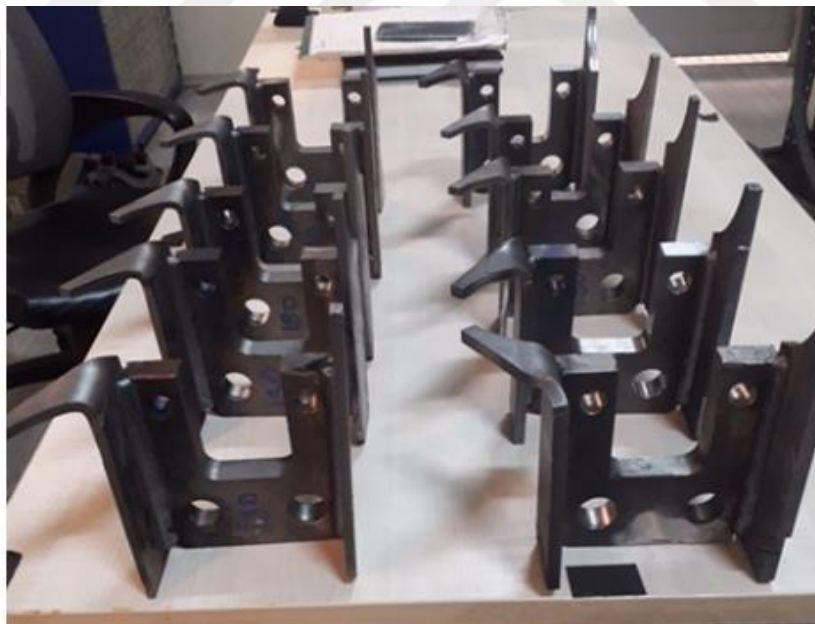


Figure 29: Welded Samples for Fatigue Testing

The MIG (Metal Inert Gas) welding technique was used for welding the parts (Figure 30). The welding current and voltage were set to 180 A and 21.6 V, respectively. The selected set values were the commonly used ones in welding of such parts in the company.



Figure 30: The MIG Welding Machine

5.2 Testing Procedure

The steps followed during the tests are given below;

- The welded samples were fixed to the vise.
- Different load values (3000N-12000N) for each sample were entered by means of the control panel. The “start” button was pressed to establish the connection between the tester and the computer.
- The hydraulic piston exerted the set load to the predetermined position of the sample (25 mm away from the weld line). The system automatically shut down itself when a break or excessive deformation of the sample took place during the test.
- The number of cycles (N) until the fracture/failure was read and recorded from the connected computer. The applied loads (F) and corresponding N values until fractures are given Table 3.

Table 3: Fatigue Test Results of the Specimens

SAMPLE NO	APPLIED FORCE, V (N)	NUMBER OF CYCLES, N	SHEAR STRESS, τ , (MPa)
1	12000	6470	207,6
2	10000	8233	173,0
3	9000	11261	155,7
4	8000	20109	138,4
5	7500	29249	129,7
6	7000	33081	121,1
7	6000	58379	103,8
8	5000	125633	86,5
9	3500	677658	60,4
10	3000	3012546	51,9

5.3 Stress Calculations for the Tested Sample

The dimensions of the tested sample (Figure 28) and load values are as follows;

- $t = 0,707*(4,5)$ mm
- $b = 115$ mm
- $l = 25$ mm
- $d=8$ mm
- $V = 3000$ N, 3500 N, 5000 N, 6000 N, 7000 N, 7500 N, 8000 N, 9000 N, 1000 N, 1200 N (Table 3)

The schematic representation of the loading geometry used in stress calculation is shown in Figure 31.

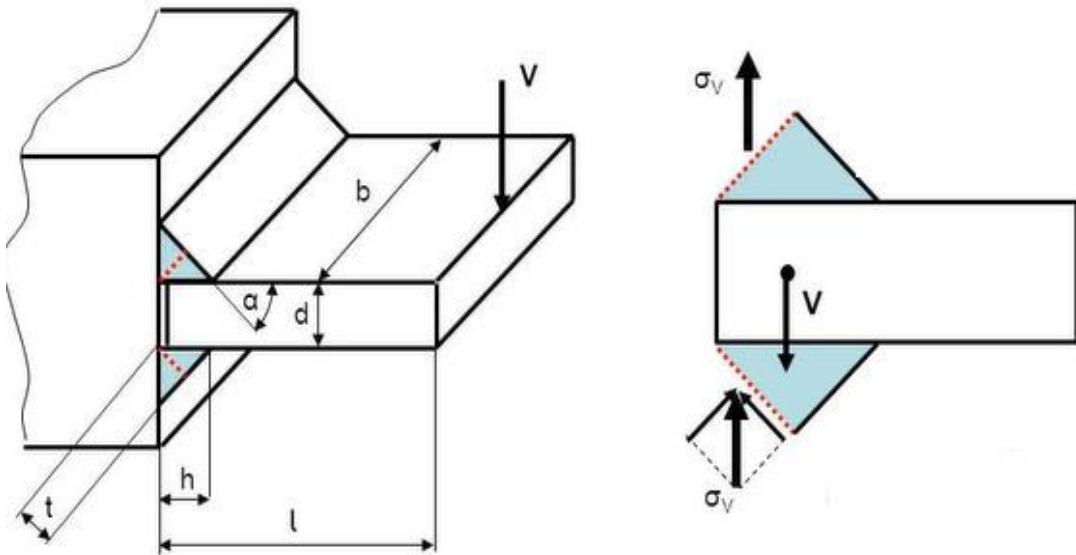


Figure 31: Fillet Welds under Primary Shear and Bending Load (t = weld width, mm, b = weld length, mm, l = lever arm length, mm, d =plate thickness, mm, V = applied force, N , τ = shear stress, MPa) [31]

The stress formulation used in the calculations is given below.

Primary shear stress (τ');

$$\tau' = \frac{V}{A} \quad (5)$$

Cross sectional area of the weld line (A);

$$A = 0,707 \cdot b \cdot t$$

Unit second moment of area of weld line (I_u);

$$I_u = \frac{bd^2}{2} \cdot \frac{1}{2} \quad (6)$$

Moment of inertia of the weld line (I);

$$I = 0,707 \cdot h \cdot I_u = 0,707 \cdot h \cdot \frac{b \cdot d^2}{4} \quad (7)$$

Normal stress (τ'');

$$\tau'' = \frac{M.c}{I} = \frac{M \cdot \frac{d}{2}}{I} \quad (8)$$

$$M = V \cdot L \quad (9)$$

Here, M is the bending moment and c is the distance to neutral axis.

Bending shear stresses (τ);

$$\tau = \sqrt{\tau'^2 + \tau''^2} \quad (10)$$

A sample calculation for 12000N load is as follows;

$$\tau' = \frac{V}{A} = \frac{12000}{0,707 \cdot 4,5 \cdot 115} = 32.8 \text{ MPa}$$

$$I_u = \frac{bd^2}{2} \cdot \frac{1}{2} = \frac{115 \cdot 8^2}{4} = 1840 \text{ mm}^3$$

$$I = 0,707 \cdot h \cdot I_u = 0,707 \cdot h \cdot \frac{b \cdot d^2}{4} = 0,707 \cdot 4,5 \cdot 1840 = 5854 \text{ mm}^4$$

$$M = V \cdot L = 12000 \cdot 25 = 300000 \text{ N} \cdot \text{mm}$$

$$\tau'' = \frac{M.c}{I} = \frac{M \cdot \frac{d}{2}}{I} = \frac{300000 \cdot \frac{8}{2}}{5854} = 204.9 \text{ MPa}$$

$$\tau = \sqrt{\tau'^2 + \tau''^2} = \sqrt{32,8^2 + 205^2} = 207.6 \text{ MPa}$$

5.4 Test Results

After the experiments were completed, a fracture analysis was performed for broken surfaces by means of optical microscopy (LEICA EZ4) with x10 magnification. The images of a broken sample and its failure surface are shown in Figure 32. It was observed that the failure took place at the weld line material of the specimens. As shown in Table 3, the strength of the welding material was reduced under repeated loads and breaks were formed in stresses (207.6-51.9 MPa) far below the ultimate tensile strength (UTS) of the welding material (360 MPa). Fatigue fracture that occurs under repeated loads started from locations where the tension was intense.

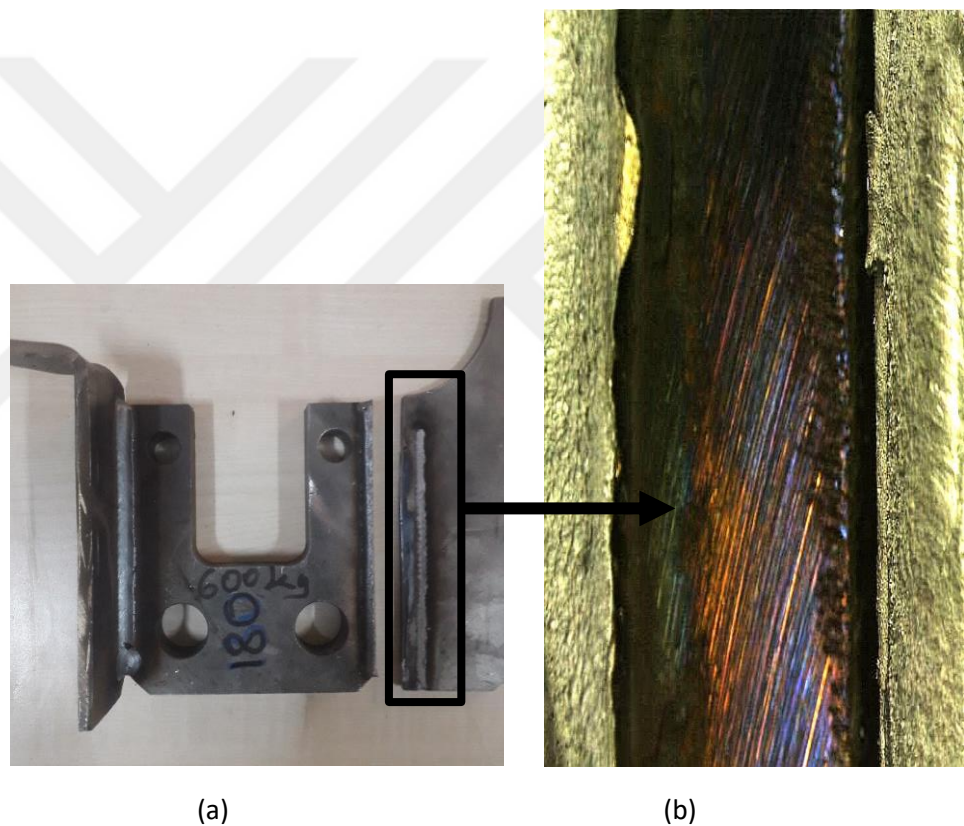


Figure 32: Test Results (a) A Fractured Sample (104 MPa) (b) Optical Image of a Failed Weld Region (“x10” Magnification)

Table 4: Fatigue Test Results of the Specimens

SAMPLE NO	APPLIED FORCE, V (N)	NUMBER OF CYCLES, N	SHEAR STRESS, τ (MPa)
1	12000	6470	207,6
2	10000	8233	173,0
3	9000	11261	155,7
4	8000	20109	138,4
5	7500	29249	129,7
6	7000	33081	121,1
7	6000	58379	103,8
8	5000	125633	86,5
9	3500	677658	60,4
10	3000	3012546	51,9

The S-N diagram obtained from the tests is presented in Figure 33 while V, τ and N are given in Table 3. It was observed that the curve became less slopy and an infinite fatigue life was almost obtained after a certain stress interval by lowering the stress value.

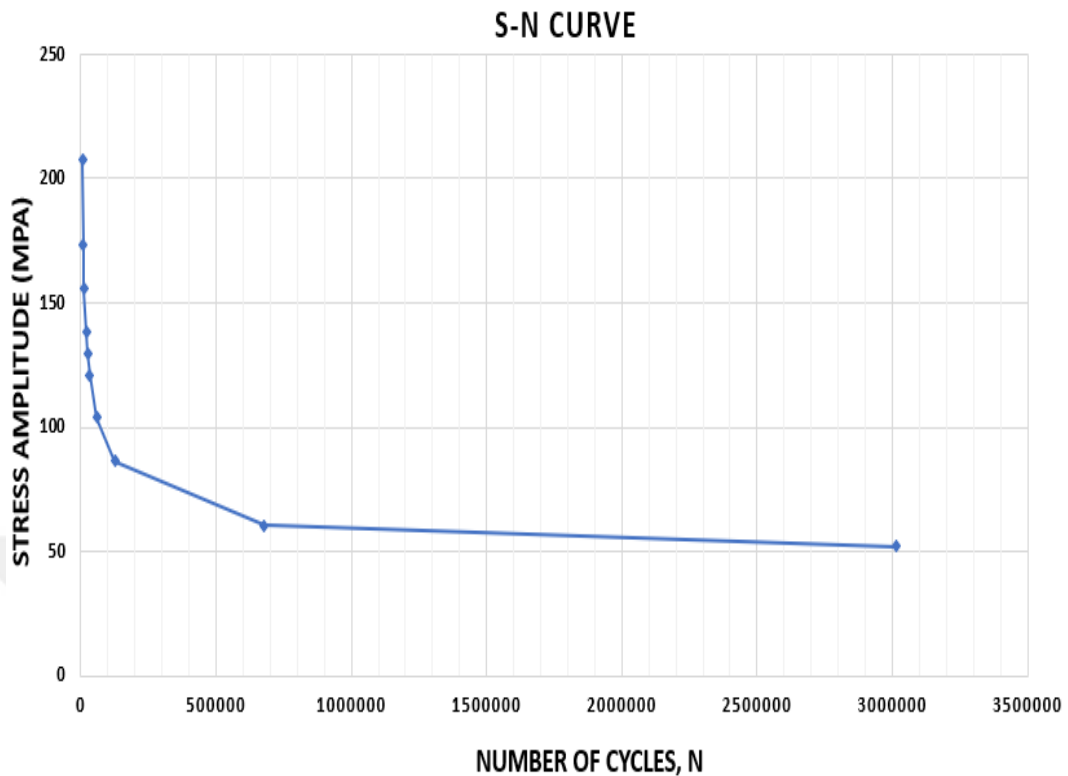


Figure 33: Stress-Strain Diagram Obtained from Fatigue Test

In order to find the S_e (endurance limit) and the corresponding N value of the tested welded specimen, the logarithmic axes ($\log(S-N)$) were introduced. The logarithmic $S-N$ graph (Figure 34) yielded the S_e of about 55 MPa at about $1 \cdot 10^6$ cycles. This number of cycles nearly corresponds to 140 shocks (loading) per day for the tested part for 20 years of service life of the bus which can be considered as a reasonable value for the rough road conditions. In Figure 34, the descending tendency of the curve even after 55 MPa yielded the need of lower loads than 3000 N to be sure of infinite life region (i.e. S_e value) of the welding material, although, $1 \cdot 10^6$ cycle, infinite life, was reached at this stress level. Moreover, the $\log(S-N)$ curve in Figure 34 indicated the need of higher load (V) than 12000 N to obtain shorter life (i.e. to reach the UTS of the material) noting that calculated 207.6 MPa stress is lower than wire material UTS of 360 MPa. Unfortunately, the hydraulic pressure and piston diameter weren't sufficient for exerting the loads above 12000 N.

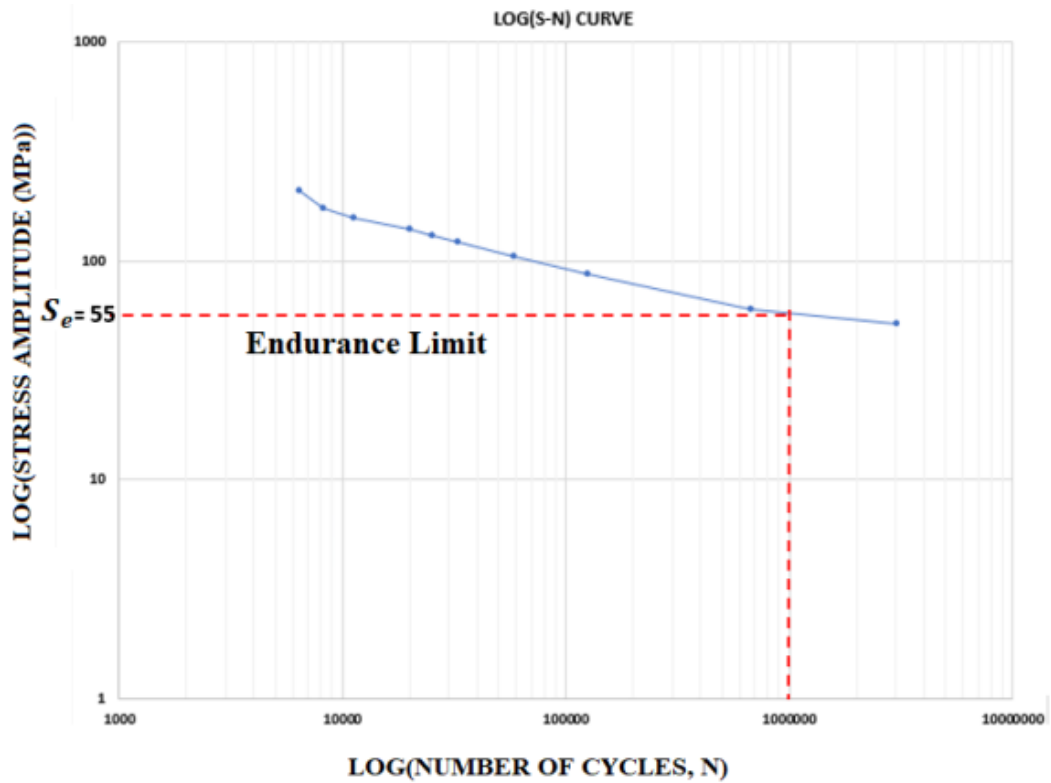


Figure 34: Endurance Limit in log (S-N) Diagram

The plastic, elastic and infinite life regions of the log (S-N) diagram, whereas theoretical background (Section 3.4.1) was presented in Figure 35. As seen from the figure, the region with N less than 10^4 cycle is interpreted as the plastic region, whereas the regions between 10^4 and 10^6 , and above 10^6 are interpreted as elastic and infinite life regions, respectively. The log (S-N) graph (Figure 35) yielded the σ_y of about 156 MPa at about 11000 cycles, pointing out the turning point of the elastic and plastic regions, whereas the actual σ_y of the welding material was 235 MPa. In this study, the plastic region of the log (S-N) curve couldn't be obtained precisely since the testing machine was not capable to exert loads higher than 12000 N (or stresses above 207.6 MPa). The UTS point of the welding material (360 MPa) was supposed to be reached at 21000 N load with 1 cycle (one stroke) in the log (S- N) curve. However, in Figure 35, 300 MPa value was reached by extrapolating the 173 and 207.6 MPa stress points towards the log S axis.

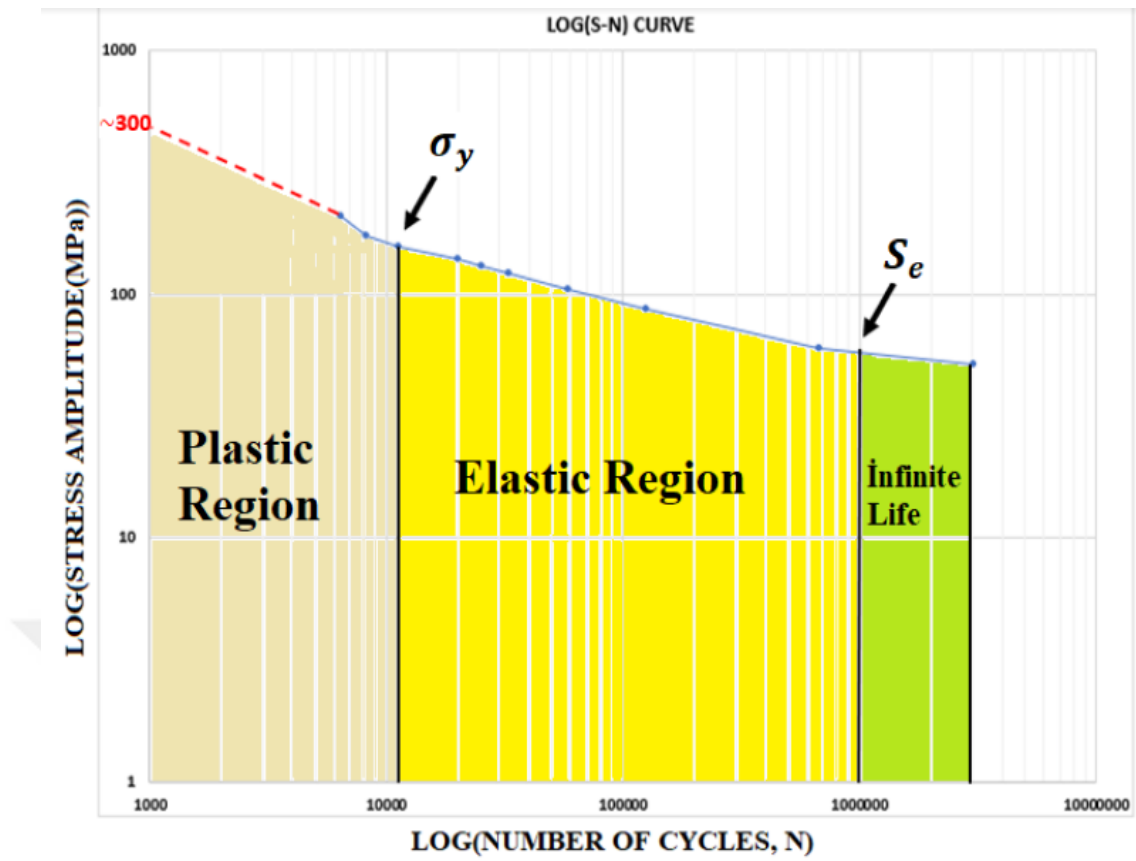


Figure 35: Plastic, Elastic and Infinite Life Regions

CHAPTER 6

6. CONCLUSION

In this study, a bending type fatigue testing machine was designed, manufactured and implemented for the welded parts of BOZANKAYA company.

The machine was hydraulically actuated and provided 3 strokes(hits)/s at a range of 3000-12000N force. The control unit was capable of setting loads as well as monitoring the number of cycles until failure. The adjustable mounting plate of the hydraulic piston and vise enabled the force application at the desired position of the specimen and mounting of various size and geometries of the parts for testing.

The performance of the machine was tested by using specimens welded at BOZANKAYA company with the MIG (Metal Inert Gas) welding technique at 180 A and 21.6 V welding parameters. The specimens failed at their welding lines (welding material) and optical microscope images verified the shear failure of the specimens under cyclic shear force loading. The plotted log(S-N) diagrams yielded S_e (endurance limit) of 55 MPa at about 1.10^6 cycles whereas 6470 cycles were experienced until failure at the maximum applied load of 12000 N. The elastic, plastic and infinite life regions of the plotted log(S-N) diagram were also presented. The log (S-N) curve plotted indicated the need of loads above 12000 N and below 3000 N to get precise plastic and infinite life regions as well as ultimate tensile strength and S_e values of the welding material of the specimens. Nevertheless, the test results indicated the acceptable performance of the machine for testing the welded parts in the company.

REFERENCES

1. Boyer, H. E., (1986). "Fatigue Testing", (Accessed: 2019.12.08),
<https://pdfs.semanticscholar.org/063f/6856e40a7a85018d1d86337ba9612bef54c9.pdf>.
2. Haidyrah, Ahmed, Newkirk Joseph and Castano Carlos. "The Minerals, Metals & Materials Society." *Technique of Nuclear Materials* (2015), 1225-1229.
3. Hitit, E., "Yorulma Deneyi", (Accessed: 2019.12.08),
http://cdn.hitit.edu.tr/mf/files/89610_20471920831.pdf.
4. Basu, S., (2012). "Resonance Bending Fatigue Testing", (Accessed: 2019.12.09),
<https://www.hbm.com/en/4264/resonant-bending-fatigue-test-on-pipes/>.
5. MNA Engineering, (2019). "WP140 Fatigue Testing Machine", (Accessed: 2019.12.09),
<http://www.mutiaranata.com/product/detail/wp-140-fatigue-testing-machine>.
6. Controls Group, "Four Point Bend Test For UTM", (Accessed: 2019.12.10),
https://www.controls-group.com/eng/asphaltbituminous-mixture-testing-equipment/four-point-bend-test-for-utm-ast-pro-and-asphaltqube_.php.
7. Blue Star Engineering & Electronics, (2019). "Fatigue Testing Machines", (Accessed: 2019.12.09),
<https://www.bluestarindia.com/e-e/testing-machines/products/fatigue-testing-machines>.
8. Instron, "Axial Torsion Fatigue Testing Machine", (Accessed: 2019.12.10),
<https://www.instron.es/es-es/testing-solutions/by-test-type/torsion/axial-torsion-fatigue>.
9. Askaynak, (2010). "Kaynaklı Birleştirmeye Uygulanacak Tahribatlı Testler Nelerdir?", (Accessed: 2019.12.12),
<https://www.askaynak.com.tr/yayinlar/bultenler/kaynakli-birlestirmeye-uygulanacak-tahribatli-testler-nelerdir>.
10. Millî Eğitim Bakanlığı, Tahribatlı Muayene, Ankara, 2011.

11. Tesko, “Tahribatlı Testler”, (Accessed: 2019.12.12), <https://www.tesko-ndt.com/kopyasi-tahribatsiz-testler>.
12. SlideShare, (2017). “Welding Inspection and Testing”, (Accessed: 2019.12.12), <https://www.slideshare.net/ArvindChavan/weld-inspection-and-testing-destructive-non-destructive-methods>.
13. BİNER, İ., “Kaynaklı Numunelerin Tahribatlı Testlerinin Güvenilirliği ve Cihaz Kalibrasyonu”, S.125-130.
14. Karadeniz Teknik Üniversitesi Ders Notu, “Tahribatsız Muayene”, (Accessed: 2019.12.12), http://www.ktu.edu.tr/dosyalar/makina_faf72.pdf.
15. Uzunsoy, D. vd. (2017). Metalik Malzemelerin Yorulma Deneyi Ders Notları.
16. Chapter 7 Introduction to Fatigue," Fracture and Fatigue Control in Structures": Applications of Fracture Mechanics, Third Edition, ed. J. Barsom and S. Rolfe (West Conshohocken, PA: ASTM International, 1999), 163-181.
17. Balıkesir Üniversitesi Ders Notları, “Yorulma Hasarları”, (Accessed: 2019.12.12), <http://w3.balikesir.edu.tr/~ay/lectures/ha/lecture6.pdf>.
18. Demirkol, M., 1991. Mekanik Metalürji Ders Notları.
19. Kayalı, S. E., Cahit, E., Dikeç, F., 1983. Metalik Malzemelerin Mekanik Deneyleri. İstanbul Teknik Üniversitesi Matbaası, 179s. İstanbul
20. Quality Magazine, “Stress Life Fatigue Testing Basics”, (Accessed: 2019.12.16), <https://www.qualitymag.com/articles/94171-stress-life-fatigue-testing-basics>.
21. NDT Resource Center, “Fatigue Properties”, (Accessed: 2019.12.16), <https://www.ndeet.org/EducationResources/CommunityCollege/Materials/Mechanical/Fatigue.htm>.
22. Science Direct, “High Cycle Fatigue”, (Accessed: 2019.12.16), <https://www.sciencedirect.com/topics/materials-science/high-cycle-fatigue>.
23. Test and Measurement World, (2016). “Low Cycle Fatigue vs High Cycle Fatigue Difference Between Low Cycle Fatigue and High Cycle Fatigue”, (Accessed: 2019.12.14), <https://www.test-and-measurement-world.com/Terminology/Low-cycle-fatigue-vs-High-cycle-fatigue.html>.

24. Insapedia, “Yorulma Kırılması Nedir?”, (Accessed: 2019.12.18), <https://insapedia.com/yorulma-kirilmesi-nedir/>.
25. Kaymaz, İ., “Yorulma Ders Notları”, (Accessed: 2019.12.13), http://muhserv.atauni.edu.tr/makine/ikaymaz/makel/lecture_notes/DERS_NO_TU_3_YORULMA.pdf.
26. SemanticScholar, “Figures and Tables”, (Accessed: 2019.12.18), <https://www.semanticscholar.org/paper/Monitoring-and-Failure-Analysis-of-Corroded-Bridge-Li-Ou/7cf8e11e5674834d15fade910f942d1090045629/figure/5>.
27. Kuntay, A., (2015). “Yorulma Teorisi Başlangıç Eğitimi”, (Accessed: 2019.12.16), https://www.bias.com.tr/imgup/Bias_Yorulma_Egitimi_Teori.pdf.
28. Comsol, “Material Fatigue”, (Accessed: 2019.12.17), <https://www.comsol.de/multiphysics/material-fatigue>.
29. Dindar, B. “Elyaf Takviyeli Kompozitlerde Nanopartikül Katkısının Yorulma, Burkulma Ve Darbe Davranışına Etkisinin Deneysel Olarak İncelenmesi” Doctoral Thesis, Pamukkale University, 2019
30. TecScience, “Fatigue Test”, (Accessed: 2019.12.18), <https://www.tec-science.com/material-science/material-testing/fatigue-test/>.
31. Juvinall, Robert C. and Marshek Kurt M. Fundamentals of Machine Component Design. ABD: John Willey & Sons, INC., 2006